Feeding of yeast cell wall extracts during a necrotic enteritis challenge enhances cell growth, survival and immune signaling in the jejunum of broiler chickens

Casey N. Johnson,[*] Mohammed M. Hashim,[†] Christopher A. Bailey,[†] James A. Byrd,[‡] Michael H. Kogut,[‡] and Ryan J. Arsenault[*,1]

*Department of Animal and Food Sciences, University of Delaware, Newark, DE 19716, USA; [†]Department of Poultry Science, Texas A&M University, College Station, TX 77843, USA; and [‡]USDA – ARS, Southern Plains Agricultural Research Center, College Station, TX 77845, USA

ABSTRACT Necrotic enteritis (NE) is one of the most common and costly diseases in the modern broiler industry, having an estimated economic impact of $6 billion dollars annually. Increasing incidents of NE have resulted from restrictions on the use of antibiotic feed additives throughout the broiler industry. As such, finding effective antibiotic alternatives has become a priority. In this study, an experimental model of NE was used, comprising a commercial infectious bursal disease virus vaccine and *Clostridium perfringens* (*C. perfringens*) inoculation. Yeast cells wall (YCW) components, β-glucan (BG), and mannoproteins (MPTs) were evaluated for their effects on disease development. Chicken-specific immunometabolic kinome peptide arrays were used to measure differential phosphorylation between control (uninfected), challenged (infected), and challenged and treated birds in duodenal, jejunal, and ileal tissues. Treatment groups included crude YCW preparation, BG, MPT, or BG+MPT as feed additives. Data analysis revealed kinome profiles cluster predominantly by tissue, with duodenum showing the greatest relative signaling and jejunum showing the greatest response to treatment. BG, MPT, and BG+MPT cluster together, separate from controls and challenge birds in each tissue. Changes in signaling resulting from the treatments were observed in cell growth and survival responses as well as immune responses. None of the treatments of disease challenge returned the profiles to control-like. This is attributable to immune modulation and metabolic effects of the treatments generating distinct profiles from control. Importantly, all the treatments are distinct from the challenge group despite being challenged themselves. Only BG+MPT treatment had a significant effect on bird weight gain compared with the NE challenge group, and this treatment had the greatest impact on gut tissue signaling in all segments. The signaling changes elicited by BG+MPT during an NE challenge were increased cell growth and survival signaling, reducing cell death, apoptosis and innate inflammatory responses, and generating compensatory signaling to reduce disease severity.

Key words: yeast cell wall, necrotic enteritis, kinome, immunity, broiler

2020 Poultry Science 99:2955–2966
https://doi.org/10.1016/j.psj.2020.03.012

INTRODUCTION

An increase in the restriction of antibiotic feed additives and growth promotors has resulted in a rise in the instances of necrotic enteritis (**NE**) in broiler flocks (Cooper and Songer, 2009). NE has been regarded as one of the most common and financially devastating bacterial diseases in the poultry industry (Songer, 1996; Cooper and Songer, 2009). Economic losses attributable to avian NE are estimated to cost the poultry industry up to $6 billion annually on a global scale (Wade and Keyburn, 2015), largely due to treatment costs and impaired growth performance (Lovland and Kaldhusdal, 2001; Immerseel et al., 2004). NE, while not a novel disease, has become an emerging threat because of legislative restrictions and the voluntary removal of in-feed antibiotics by growers, high-density housing conditions, and the reuse of poultry litter (Kaldhusdal et al., 1999; Lee et al., 2011).

Clostridium perfringens (***C. perfringens***), a commensal, gram-positive, spore-forming anaerobe, is reported as the causative agent of NE; however,

Received October 17, 2019.
Accepted March 4, 2020.

[1]Corresponding author: rja@udel.edu

predisposing factors must be present in order for the disease to manifest (Songer, 1996; Shimizu et al., 2002; McReynolds et al., 2004). These predisposing factors can include coccidiosis, infectious bursal disease virus (**IBDV**), and diets containing poorly digestible nonstarch polysaccharides such as wheat, rye, oats, or barley (Choct and Annison, 1992; McReynolds et al., 2004; Teirlynck et al., 2009). It is hypothesized that these predisposing factors cause damage to the epithelial lining of the small intestine and increase intestinal content viscosity, providing an ideal environment for the growth and proliferation of *C. perfringens* (Annett et al., 2002; Cooper and Songer, 2009). As broiler chickens are inevitably going to be exposed to *C. perfringens* as well as at least some of the predisposing factors, it has become necessary to find new ways of mitigating NE development.

The yeast cell wall (**YCW**) of *Saccharomyces cerevisiae* has been studied as a possible antibiotic alternative (Ha et al., 2006; M'Sadeq et al., 2015; Hashim et al., 2018). Products containing YCW components are currently used as feed additives in production animals and have been shown to have a positive impact on animal growth and performance (Hashim et al., 2018). Current evidence points to YCW components imparting a modulatory effect on the immune system in the intestinal tract of poultry. YCW components are ligands for immune receptors and, as such, impart an immune effect that has been hypothesized to mediate immune responses to pathogens such as *C. perfringens*. Two of the main components of YCW believed to impart an immune effect are β-glucan (**BG**) and mannoproteins (**MPT**), and these are thought to contribute to the disease mitigation. BG is a highly conserved structural component of cell walls in yeast, other fungi, or seaweed which has been shown to be productive immunologically (Novak and Vetvicka, 2008; Soltanian et al., 2009). BG has been shown to impact cytokine expression in broiler chicks when used as a feed additive, indicating immunological impacts (Cox et al., 2010). In addition, immune receptors (Dectin-1, complement receptor [**CR3**], and Toll-like receptors [**TLRs**] 2 and 6) and immune cells (macrophages, neutrophils, monocytes, natural killer cells, and dendritic cells) have been shown to respond to BG (Novak and Vetvicka, 2008). MPTs are glycoproteins that contain 15–90% mannose by weight; they make up part of the yeast cell wall and are linked to other cell wall components such as BG and chitin (Cohen and Ballou, 1981). MPTs have a molecular mass of between 100 and 200 kDa and comprise approximately 40% of the dry weight of the cell wall (Lipke and Ovalle, 1998). MPTs have been shown to be immunemodulators with immune-altering activities (Ha et al., 2006) and immunostimulatory enhancing dendritic cell and T-cell activity (Pietrella et al., 2006).

Virtually all immune signaling and many metabolic pathways contain key components that are regulated by protein kinases. Kinomics involves the analysis of phosphorylation, catalyzed by protein kinases, the predominant posttranslational modification of proteins in eukaryotes, which plays a key role in mediating most cellular signaling cascades. As phosphorylation represents a pivotal mechanism for regulation of biological processes, kinases are undeniably one of the most biologically significant host proteins (Jalal et al., 2007). Phosphorylation regulates a multitude of protein functions and behaviors including activity, stability, cellular localization, and interacting partners (Jalal et al., 2007). Regulation of protein function through phosphorylation is observed in virtually every cellular process including metabolism, cell division, apoptosis, and signal transduction (Hunter, 1995; Jalal et al., 2007, 2009). The reversible nature of the modification makes phosphorylation a critical feature and an effective mechanism for regulation of protein behavior (Jalal et al., 2007). The development of the species-specific kinome peptide array has provided an invaluable tool for exploring host responses to diseases such as NE via phosphorylation-mediated signaling (Arsenault and Kogut, 2013).

Owing to the increased incidence of NE in modern broiler flocks and its cost to the industry, a need for alternative antimicrobial control of *C. perfringens* has become necessary. A better understanding of host response needs to be established to elucidate the changes that result in NE thereby enabling researchers to more efficiently develop control and prevention strategies. Taking an immunometabolic approach to this problem and exploring the biological changes occurring via phosphorylation mediated signal transduction pathways will reveal potential targets for treatment and prevention options. In this article, we report the changes in signal transduction due to YCW fractions in an experimental model of NE that predominantly impact cell growth, survival and innate immune responses.

MATERIALS AND METHODS

Ethics Statement

The study was conducted at the Southern Plains Agricultural Research Center, Agricultural Research Service, United States Department of Agriculture, and the animal use protocol was approved by the Animal Care and Use Committee at the Southern Plains Agricultural Research Center. All experiments were conducted according to guidelines established by the USDA Animal Care and Use Committee, which operates in accordance with established principles (National Research Council (US) Committee for the Update of the Guide for the Care and Use of Laboratory Animals, 2011).

Experimental Design

A basal industry-type broiler starter diet was prepared to meet or exceed the 1994 National Research Council's Nutrient Requirements of Poultry (Tables 1 and 2). These diets were fed as crumbled pellets. A total of 240 Ross 308 broiler chicks were distributed among 2 Petersime battery brooder units (48 pens; 6 levels, 8 pens

per level, 5 birds per pen). A total of 6 treatments (Table 3) were randomly assigned to pens such that each treatment was represented at least once for any given level of pens.

This study was conducted to evaluate purified YCW fractions and a crude YCW preparation on starter broiler performance. The YCW product contained 23.5% mannoproteins and 23.8% glucans, it is important to note that crude YCW can have significant quantities of other cell wall components remaining in the final product, although cytosolic components had been removed. The YCW, MPT, and BG preparations were provided by (Phileo-Lesaffre Animal Care, Milwaukee, WI).

All birds of 6 treatments were immunocompromised with infectious bursal disease vaccine (Schering Plough Animal Health, Millsboro, DE) on day 10. The vaccine was administered at 10× the manufacturer's recommended dose via the ocular route to immunocompromise the chicks (McReynolds et al., 2004). On day 16 and 17, all groups, except nonchallenged control, were challenged with *C. perfringens* (10^7 cfu/mL, 3 mL oral gavage). Feed and water were provided ad libitum. Feed and body weight data were recorded on days 1, 10, 16, and 21. The study was terminated on day 21.

Administration and Isolation of C. perfringens

C. perfringens–containing medium was provided by the ARS, Southern Plains Agricultural Research Center, USDA. The isolation and preparation of *C. perfringens* were as described in the article by McReynolds et al., 2004. The *C. perfringens* pathogen was a combination of 4 type A field isolates from 3 different regions (Georgia, Texas, and Virginia). One gram of the gastrointestinal contents of birds diagnosed with necrotic enteritis was taken to an anaerobic chamber and placed into 10 mL of liquid thioglycollate medium (Becton Dickinson Co., Sparks, MD) and incubated for 24 h at 37°C. These isolates were cultured individually, combined, and administered to the birds.

Sampling and Tissue Collection

Tissue samples from the duodenum, jejunum, and ileum of 3 birds per treatment were collected at day 21, flash-frozen in liquid nitrogen, and sent to the University of Delaware to conduct kinome analysis using chicken-specific peptide array protocol.

Table 1. Starter diet composition.

Ingredient name	Pounds	Percent
TAMU CORN #21	537.59	58.434
TAMU SOYBEAN ML48%	317.34	34.493
DL-MET98	2.13	0.231
LYSINE HCL	1.63	0.177
AV BLEND 8500	25.35	2.755
LIMESTONE	14.36	1.561
BIOFOS 16/21P	14.14	1.537
SALT	4.71	0.512
TAMU TRACE MINERALS	0.46	0.05
TAMU VITAMINS	2.3	0.25
Total	920	100

Table 2. Nutrient composition.

Nutrient name	Amount	Units
Dry matter	90.096	PCT
Moisture	9.904	PCT
Protein	22	PCT
Crude fat	5.32	PCT
Crude fiber	2.631	PCT
Calcium	0.95	PCT
Phosphorus	0.705	PCT
AV phosphate	0.45	PCT
ME poultry, kcal/kg	3,050.00	KCAL/KG
ME poultry, kcal/lb	1,386.36	KCAL/LB
Xanthophyll, mg/kg	9.934	MG/KG
Available methionine	0.532	PCT
Available total sulfur amino acids	0.825	PCT
Availabile lysine	1.19	PCT
Methionine	0.56	PCT
Total sulfur amino acids	0.921	PCT
Lysine	1.31	PCT
Tryptophan	0.264	PCT
Threonine	0.821	PCT
Arginine	1.453	PCT
Glycine	0.9	PCT
Linoleic acid	2.112	PCT
Electrolytes	206.57	MEQ/KG
Sodium	0.22	PCT
Potassium	0.86	PCT
Chloride	0.387	PCT

Chicken-Specific Immunometabolic Kinome Peptide Array

Peptide array protocol carried out as previously described and summarized in the following section (Arsenault et al., 2017). Forty milligrams of tissue samples were used for the kinome peptide array protocol. Samples were homogenized by a Bead Ruptor 24 homogenizer (Omni International, Kennesaw, GA) in 100 µL of lysis buffer containing protease inhibitors. Homogenized samples were then mixed with an activation mix containing ATP and applied to peptide arrays. Arrays were incubated in a humidity chamber at 37°C with 5% CO_2, allowing kinases to phosphorylate their target sites. Samples were then washed off the arrays, and a florescent phosphostain was applied. Stain not bound to phosphorylated sites was removed by a destaining process. Arrays were then imaged using a Tecan PowerScanner microarray scanner (Tecan Systems, San Jose, CA) at 532 to 560 nm with a 580-nm filter to detect dye fluorescence.

Array images were then gridded using GenePix Pro software (Molecular Devices, San Jose, CA), and the spot intensity signal was collected, ensuring peptide spots were correctly associated with their phosphorylation site. Greater intensity florescence correlates to greater phosphorylation at the target site. Florescent intensities for treatments were then compared with those for controls using a data normalization program, Platform for Intelligent, Integrated Kinome Analysis (Trost et al., 2013). The resulting data

Table 3. Experimental groups in trial.

Experimental groups	Group short form	Treatment level
Nonchallenged control	Control	0 ppm
Challenged control	NE	0 ppm
Semi-purified yeast cell wall + challenge	YCW	250 ppm
Beta glucan + challenge	BG	108.4 ppm
Mannoprotein + challenge	MPT	117.3 ppm
Beta glucan + mannoprotein + challenge	BG+MPT	108.4 + 117.3 ppm

Abbreviations: BG, β-glucan; MPT, mannoproteins; NE, necrotic enteritis; YCW, yeast cells wall.

output was then used in downstream applications such as Search Tool for the Retrieval of Interacting Genes/Proteins (Szklarczyk et al., 2015) and Kyoto Encyclopedia of Genes and Genomes (Kanehisa et al., 2017) databases used to pinpoint changes in protein-protein interactions and signal transduction pathways.

RNA Extraction for Quantitative Real-time Reverse Transcription Polymerase Chain Reaction

A piece of tissue (30–40 mg) was placed in a 2-mL prefilled tube containing 1.5-mm high-impact zironium beads (TriplePure M-Bio Grade; Benchmark Scientific). Lysis buffer (350 μL; RNeasy Mini Kit; Qiagen) was added, and the sample was homogenized in the BeadBug for 2 min on the maximum speed. Tissue homogenization was performed using a BeadBug microtube homogenizer (Benchmark Scientific, Edison, NJ). Total RNA was then isolated from the homogenized samples according to the manufacturer's instructions, eluted with 50 μL of RNase-free water, and stored at −80°C until quantitative real-time reverse transcription polymerase chain reaction (**qRT-PCR**) analyses were performed.

Primers and probes for cytokines, chemokines, and 28S RNA-specific amplification have been previously described (Kaiser et al., 2000; Kogut et al., 2003; Swaggerty et al., 2008). The qRT-PCR was performed using the TaqMan one-step RT-PCR master mix reagents (Applied Biosystems, Branchburg, NJ). Amplification and detection of specific products were performed using the Applied Biosystems 7,500 Fast Real-Time PCR System with the following cycle profile: one cycle of 48°C for 30 min and 95°C for 20 s and 40 cycles of 95°C for 3 s and 60°C for 30 s. Quantification was based on the increased fluorescence detected by the 7,500 Fast Sequence Detection System due to hydrolysis of the target-specific probes by the 5′ nuclease activity of the *rTth* DNA polymerase during PCR amplification.

Data Analysis

Body weight, weight gain, phase feed-to-gain ratio (P-F:G), cumulative feed-to-gain ratio (C-F:G), and feed conversion ratio data were analyzed as a one-way ANOVA using SPSS's general linear model. Outlier values were excluded from challenge control and YCW groups. Because of unequal number of replicates per treatment, type I error was not guaranteed, and thus Duncan's and Tukey HSD tests were used to separate means $\alpha \leq 0.05$. Each vertical level of pens was considered a bloc for statistical purposes; each treatment was represented in each level.

Fold change was calculated using the double-delta C_t ($\mathbf{\Delta\Delta}\boldsymbol{C_t}$) method (Yuan et al., 2006). To regulate the scales of upregulated and downregulated genes, we have converted the decimal fold changes, which represent decreases in gene expression relative to control, into negative fold changes. This is calculated as fold change = $-1/x$, where x is the relative decreased, decimal, fold change in treatment compared to control. For example, a $\Delta\Delta C_t$ fold change value of 0.5 would become -2 ($-1/0.5 = -2$). Without this true fold change calculation, an increase in gene expression is represented as any value from 1 to infinity, and a decreased gene expression value could only be represented by < 1 to 0. In addition, this true fold change calculation brings the PCR data into a similar presentation of fold change as the kinome data.

RESULTS AND DISCUSSION

Bird Performance

Bird weights for each group were taken at day 1 (placement), and weight gain was subsequently recorded at day 10, pre-IBDV vaccination, day 16, pre-*Clostridium perfingens* challenge, and day 21, post-*C. perfingens* challenge (Table 4–6). Statistically significant differences in weight gain were determined using Protected Duncan's test ($P < 0.05$). There were no statistically significant differences in weight gain between treatment groups at days 10 and 16 (data not shown). At day 21, the *C. perfringens* challenge group showed statistically significantly less weight gain than the control and BG+MPT groups (Table 6). Control and BG+MPT showed no statistically significant difference in weight gain, while the remaining groups (YCW, BG, MPT) were not statistically significantly different from either the challenged group, the control group, or the BG+MPT group. The weight gain recovery seen in the BG+MPT group indicates that a physiological shift has occurred in the birds because despite being challenged in the same manner, the birds being fed the diet

Table 4. Day-10 prevaccination performance data.

Measurement	Control	NE	YCW	BG	MPT	BG+MPT
BW	265 ± 15	255 ± 18	260 ± 9	260 ± 14	249 ± 20	257 ± 10
BWG	220 ± 15	210 ± 18	215 ± 9	214 ± 14	203 ± 20	212 ± 9
P-F:G	1.19 ± 0.04	1.19 ± 0.02	1.19 ± 0.02	1.19 ± 0.03	1.19 ± 0.04	1.19 ± 0.03
IFCR	0.98 ± 0.02	0.98 ± 0.03	0.98 ± 0.02	0.98 ± 0.02	0.98 ± 0.03	0.98 ± 0.02
PI	218 ± 22	215 ± 13	219 ± 8	219 ± 16	206 ± 32	210 ± 22
Pre-V Mort	2.5 ± 7.1	0	0	0	2.5 ± 7.1	2.9 ± 7.6

Values in the table are given as mean ± standard deviation; one-way ANOVA.

Abbreviations: BG, β-glucan; BW, body weight; BWG, body weight gain; C-F:G, cumulative feed-to-gain ratio; IFCR, individual feed conversion ratio; MPT, mannoproteins; NE, necrotic enteritis; P-F:G, phase feed-to-gain ratio; PI, performance index; P-Mort, phase mortality; YCW, yeast cells wall.

supplemented with BG+MPT were able to gain weight as well as the nonchallenged group. Thus, the BG+MPT treatment was the most effective in reducing the growth inhibition burden and restoring weight gain after the NE challenge.

Heatmaps and Clustering

Duodenum, ileum, and jejunal samples were collected at day 21 after hatch and analyzed by kinome peptide array analysis. The heatmap displays the complete kinome data set, the colored lines representing individual peptides and their phosphorylation state and the columns representing treatment groups and tissues (Figure 1). Red represents increased relative phosphorylation while green indicates less phosphorylation relative to the aggregate of the data set. The treatment groups are labeled on the X-axis. The dendrogram above the heatmap shows the hierarchical clustering of the groups. Within the dendrogram, shorter lines show greater similarity between groups while longer lines show greater difference.

In Figure 1, primary clusters from left to right are duodenum, ileum, and jejunum, clustering primarily by tissue type. This result was to be expected, as each segment of the gut, being physiologically distinct, would have a different protein phosphorylation profile regardless of experimental condition. This tissue difference is especially clear when we observe that the duodenum had a generally higher peptide phosphorylation status than ileum and jejunum, as indicated by the red color within the duodenum columns of Figure 1. The exception to this primary clustering is the control jejunal tissue, which is separated from the rest of the jejunal cluster and located between the duodenal and ileal clusters. In addition, within the jejunum treatment cluster, the challenge group is most separated from the treatment groups, especially from MPT and BG+MPT. Within the tissue clusters, the challenge group clusters separately from the tissue collected from birds treated with the various yeast compounds and challenged. The exception to this trend was the YCW treated groups; they also clustered separately in duodenum and ileum. As the various YCW compounds showed a more consistent response in the jejunum and the most distinct separation from the untreated control tissue kinotype, perhaps because the jejunum is a major site of activity for YCW compounds (Iji et al., 2001; M'Sadeq et al., 2015), we further analyzed in detail the kinome data from jejunal tissue.

Biological Process Analysis

We then considered the individual peptide phosphorylation results generated by the Platform for Intelligent, Integrated Kinome Analysis 2 online analysis platform (Trost et al., 2013). These data are a series of fold changes and significance values for each peptide on the array from each sample analyzed. These values were generated by comparing treated or challenged or both tissue array outputs to nonchallenged control array outputs. The Search Tool for the Retrieval of Interacting Genes/Proteins protein-protein interaction database (Szklarczyk et al., 2015) generates GO Biological

Table 5. Day-16 prechallenge performance data.

Measurement	Control	NE	YCW	BG	MPT	BG+MPT
BW/B	538 ± 40	510 ± 50	531 ± 34	540 ± 35	539 ± 31	549 ± 19
WG/B	273 ± 27	255 ± 32	271 ± 26	280 ± 27	291 ± 34	292 ± 14
P-F:G	1.44 ± 0.07^{b}	1.44 ± 0.09^{b}	1.37 ± 0.03^{a}	1.37 ± 0.05^{a}	1.36 ± 0.02^{a}	1.34 ± 0.03^{a}
C-F:G	1.32 ± 0.04^{b}	1.32 ± 0.04^{b}	1.29 ± 0.02^{a,b}	1.29 ± 0.04^{a,b}	1.28 ± 0.02^{a}	1.27 ± 0.02^{a}
IFCR	1.21 ± 0.02^{c}	1.20 ± 0.03^{c,b}	1.18 ± 0.01^{a,b}	1.18 ± 0.02^{a,b}	1.17 ± 0.01^{a}	1.17 ± 0.01^{a}
PI	249 ± 32	235 ± 36	257 ± 19	262 ± 21	257 ± 27	262 ± 29
P-Mort	0	3.3 ± 8.2	0	0	0	0
C-Mort	3.3 ± 8.2	2.5 ± 7.1	0	0	2.5 ± 7.1	2.9 ± 7.6

Means within a row with no common superscript alphabet differ significantly ($P < 0.05$) using protective Duncan's test. Values in the table are given as mean ± standard deviation; one-way ANOVA.

Abbreviations: BG, β-glucan; BW, body weight; BWG, body weight gain; C-F:G, cumulative feed-to-gain ratio; IFCR, individual feed conversion ratio; MPT, mannoproteins; NE, necrotic enteritis; P-F:G, phase feed-to-gain ratio; PI, performance index; P-Mort, phase mortality; YCW, yeast cells wall.

Table 6. Day-21 post-challenge performance data.

Measurement	Control	NE	YCW	BG	MPT	BG+MPT
BW/B	843 ± 67*	751 ± 71	816 ± 67	792 ± 75	801 ± 54	855 ± 65*
WG/B	305 ± 31^{a}	240 ± 43^{b}	285 ± 43^{ab}	252 ± 55^{ab}	262 ± 44^{ab}	306 ± 56^{a}
P-F:G	1.46 ± 0.10	1.64 ± 0.21	1.58 ± 0.18	1.73 ± 0.29	1.69 ± 0.19	1.59 ± 0.20
C-F:G	1.38 ± 0.06	1.42 ± 0.07	1.38 ± 0.05	1.41 ± 0.06	1.40 ± 0.03	1.38 ± 0.07
IFCR	1.30 ± 0.04	1.33 ± 0.05	1.30 ± 0.04	1.33 ± 0.05	1.31 ± 0.02	1.30 ± 0.07
PI	286 ± 42	246 ± 45	262 ± 51	234 ± 44	225 ± 50	243 ± 50
P-Mort	0	0	6.7 ± 16.3	13.1 ± 15.3	16.3 ± 14.8	14.3 ± 19.0
C-Mort	3.3 ± 8.2	2.5 ± 7.1	6.7 ± 16.3	12.5 ± 14.9	17.5 ± 16.7	17.14 ± 18.0

Means within a row with no common superscript alphabet differ significantly ($P < 0.05$) using Protected Duncan's test. Values in the table are given as mean ± standard deviation; one-way ANOVA.

*$P = 0.08$ and Tukey HSD P value = 0.075 between Ch-Ctrl and T6.

Abbreviations: BG, β-glucan; BW, body weight; BWG, body weight gain; P-F:G, phase feed-to-gain ratio; C-F:G, cumulative feed-to-gain ratio; IFCR, individual feed conversion ratio; MPT, mannoproteins; NE, necrotic enteritis; PI, performance index; P-Mort, phase mortality; YCW, yeast cells wall.

Process terms and a false discovery rate that indicates the likelihood of a biological process being truly represented in the data and not generated by random chance. The top 100 biological processes for each group were compared to find the differences between the lists generated for each experimental group. The biological processes that were distinct for each group were considered along with their associated false discovery rate. Of particular interest was what changed between groups, that is, what was significant in one group and insignificant in another, especially between the challenge group and the BG+MPT group. We considered the comparison of these 2 groups to be the most interesting given that the combination of BG+MPT in NE-challenged birds was the only treatment to restore weight gain to control bird levels and that the BG+MPT group clustered furthest from the challenge group when observing the kinotypes (Figure 1). We analyzed the GO terms

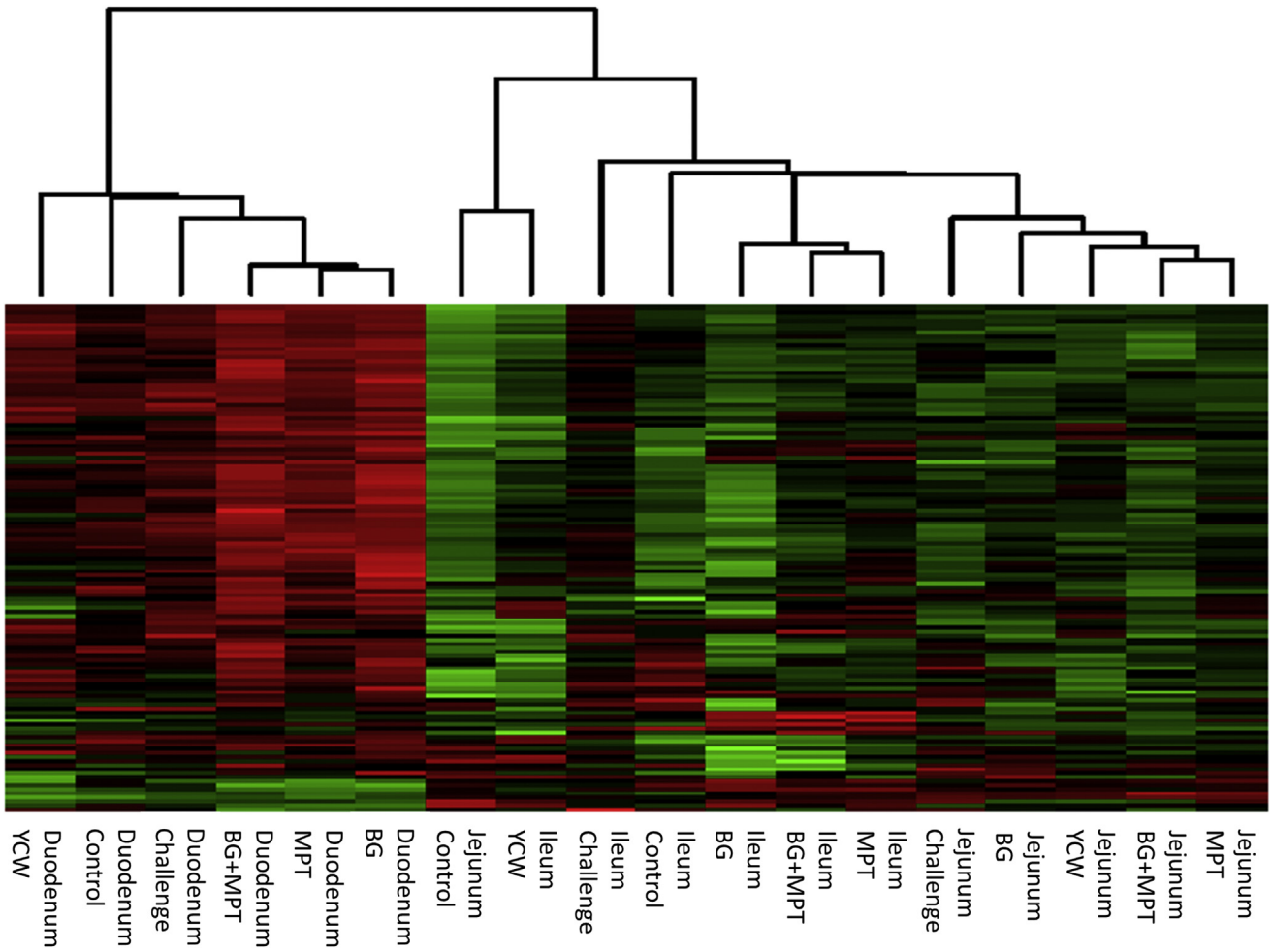

Figure 1. Heatmap displaying changes in phosphorylation status of peptides in both control and experimental groups relative to the aggregate of the postnormalization complete data.

Table 7. Biological processes not common to each group from the top 100 biological processes for each experimental group from STRING analysis.

		Challenge		YCW		Beta glucan		MPT		BG+MPT	
Pathway ID	Pathway description	#	FDR	#	FDR	#	FDR	#	FDR	#	FDR
GO.0060548	Negative regulation of cell death	62	1.1E-27								
GO.0051240	Positive regulation of multicellular organismal process	76	2E-29								
GO.0051239	Regulation of multicellular organismal process	98	6.82E-29								
GO.0014070	Response to organic cyclic compound	59	5.97E-28								
GO.1901701	Cellular response to oxygen-containing compound			73	6.11E-34						
GO.0009891	Positive regulation of biosynthetic process			100	7.13E-31						
GO.0031328	Positive regulation of cellular biosynthetic process			99	6.88E-31						
GO.0002755	MyD88-dependent toll-like receptor signaling pathway					31	5.75E-33				
GO.0034134	Toll-like receptor 2 signaling pathway					29	2.03E-31				
GO.0034142	Toll-like receptor 4 signaling pathway					32	1.27E-31				
GO.0018193	Peptidyl-amino acid modification							74	1.18E-31		
GO.0032868	Response to insulin							46	2.47E-31		
GO.0032147	Activation of protein kinase activity									51	3.19E-34
GO.0042981	Regulation of apoptotic process									95	1.24E-33
GO.0002684	Positive regulation of immune system process			73	2.45E-33	70	2.28E-31	72	2.29E-31	81	7.16E-39
GO.0045860	Positive regulation of protein kinase activity			57	4.01E-34	55	1.46E-32	55	3.23E-31	62	4.1E-38
GO.0051347	Positive regulation of transferase activity			64	1.34E-34	62	3.14E-33	64	1.29E-33	70	4.18E-39
GO.0044344	Cellular response to fibroblast growth factor stimulus	36	3.94E-30							44	1.18E-35
GO.0008543	Fibroblast growth factor receptor signaling pathway	34	2.01E-29							42	1.75E-35
GO.0002758	Innate immune response-activating signal transduction	38	7.49E-29	43	8.58E-31	44	2.25E-32	45	1.96E-32		
GO.0038179	Neurotrophin signaling pathway	51	2.24E-41	55	4.79E-41					60	6.43E-46
GO.0018108	Peptidyl-tyrosine phosphorylation			37	7.13E-31			42	6.23E-37		
GO.0048518	Positive regulation of biological process	147	3.84E-31			172	3.13E-32	182	6.43E-34	189	4.13E-37
GO.0031349	Positive regulation of defense response	45	1.89E-29			52	1.09E-32				
GO.0045089	Positive regulation of innate immune response					46	1.94E-31	47	2.14E-31		
GO.0010941	Regulation of cell death	77	1.03E-27	93	8.7E-32			93	2.12E-30	100	4.11E-35
GO.0032879	Regulation of localization			117	5.14E-33					128	3.75E-38
GO.0071900	Regulation of protein serine/threonine kinase activity			57	4.01E-34	54	1.51E-31			60	5.03E-36
GO.0009725	Response to hormone	66	2.41E-32	74	1.22E-32	72	1.41E-31	74	1.63E-31		
GO.0007165	Signal transduction	141	6.56E-31					171	9.08E-32	177	2.18E-34
GO.0002224	Toll-like receptor signaling pathway					35	8.81E-33	34	1.71E-30		

The top 100 most significant (FDR) biological processes from lists generated by STRING for each group (after imputing statistically significantly differentially phosphorylated peptides per treatment). Only processes that were not common to all groups were included to look for changes in biological processes between groups. Results were then sorted to highlight what processes were unique in each group or common except for the BG+MPT group. Highlighted are biological processes that are different between the NE challenge group and the BG+MPT group. # refers to the number of significant peptides in the kinome data set within the given pathway.

Abbreviations: BG, β-glucan; FDR, false discovery rate; MPT, mannoproteins; NE, necrotic enteritis; YCW, yeast cells wall.

Table 8. Peptides in "negative regulation of cell death" showing opposite differential phosphorylation relative to control in challenge and BG+MPT.

UniProt ID	Protein name	Human site	Chicken site	Challenge		BG		MPT		YCW		BG+MPT	
				FC	*P* value	FC	*P* value	FC	*P* value	FC	*P* value	FC	*P* value
P00533	EGFR	T693	T618	1.031	0.001	1.033	0.009	1.060	0	1.037	0.002		
P12931	SRC	S17	S17	1.032	0.037							−1.030	0.016
P17252	KPCA	T497	T499	−1.032	0.029					−1.055	0	1.025	0.023
P31749	AKT1	T308	T74	−1.045	0.020							1.054	0.008
P49841	GSK3B	Y216	Y186	1.075	0.008	1.077	0.001			−1.090	0	−1.056	0.010
P51692	STA5B	Y740	Y741	−1.120	0.001	−1.078	0.001	−1.030	0.046	−1.078	0		
P51692	STA5B	Y699	Y700	−1.036	0.003			1.041	0			1.054	0.003
Q13131	AAPK1	S172	S174	−1.052	0.001					−1.022	0.018	1.032	0.0178
Q14289	FAK2	Y580	Y584	1.039	0.004	1.048	0.002	1.039	0.007	1.060	0.028		
Q16288	NTRK3	Y516	Y409	−1.041	0.007					1.061	0.011	1.032	0.043
Q16654	PDK4	S369	S363	−1.153	0	−1.095	0.001	−1.130	0	−1.105	0	1.029	0.037
Q9NZJ5	E2AK3	T982	T959	1.045	0.006							−1.040	0.002

A *P* value of 0.05 was used to determine significance. Nonsignificant values have been omitted.
Abbreviations: BG, β-glucan; FC, fold change; MPT, mannoproteins; YCW, yeast cells wall.

generated from the kinome data related to biological processes for these 2 experimental groups. Highlighted in Table 7 are the function-specific biological processes that appear in only one of the 2 groups, either challenge or BG+MPT group, and are not generic cellular responses. The GO term biological processes that are distinct between the challenge group and the BG+MPT group relate to innate immune response and cell death or apoptosis (Table 7). The GO term "negative regulation of cell death" only appears in the challenge kinome data, "regulation of apoptotic process" only appears in the BG+MPT kinome data, and "innate immune response activing signal transduction" appears in all groups except the BG+MPT kinome data. The other terms that show these clear distinctions between challenge and BG+MPT are generic terms that do not provide specific biological function information, such as "positive regulation of multicellular organismal process" or "activation of protein kinase activity", thus these are not highlighted in Table 7 and were not considered further for analysis. These cell death or apoptosis and immune response processes are of particular interest when we consider that NE is characterized by necrotic lesion formation and tissue death in the small intestine of broilers (Lee et al., 2011), perhaps due to an overactive innate inflammatory response (Sarson et al., 2009).

Looking into the proteins associated with the GO term biological processes and the protein phosphorylation sites represented on the array showing significant differential phosphorylation, one can begin to understand what specific physiological changes are occurring between the challenge and the BG+MPT groups. These 3 biological processes that were different between the challenge group and the BG+MPT group were considered more closely by generating the list of peptides associated with the processes that had changed in each group. Again, we trimmed the list to find what was different between the challenge group and the BG+MPT group. We have included the complete data set (untrimmed) of peptides associated with the biological processes as supplementary tables (Supplementary Tables 1–3). Table 8 shows the peptides that are uniquely significant or phosphorylated in the opposite direction (i.e., increased in one group, down in the other group) between challenge and BG+MPT treated and are members of the "negative regulation of cell death" biological process. The complete list of significantly differentially phosphorylated peptides implicated in negative regulation of cell death can be found in Supplementary Table 1. We can see that most of the differences between the 2 experimental groups are because of the peptides displaying less phosphorylation relative to control in the challenge group. The specific functional changes induced by a change in phosphorylation of the individual peptides in Table 8 provide an indication of what alterations are occurring in the tissue. Phosphorylation of RAC-alpha serine/threonine-protein kinase (AKT1) T74 (Human T308) (Ma et al., 2008), Signal transducer and activator of transcription 5B (STAT5B) Y700 (Human Y699) (Fox et al., 2008), 5′-AMP-activated protein kinase catalytic subunit alpha-1 (AAPK) 1 S174 (Human S172), and NT-3 growth factor receptor (NTRK3) Y409 (Human Y516) (Postigo et al., 2002) all lead to either increased growth, increased cell survival, or increased transcription; all are increased in the BG+MPT treated group and show reduced phosphorylation in challenge. Eukaryotic translation initiation factor 2-alpha kinase 3 (E2AK3) T959 (Human T982) shows increased phosphorylation due to challenge; this sites' function is to reduce translation and is linked to stress (Kebache et al., 2004). Pyruvate kinase 2 (FAK2) Y584 (Human Y580) shows increased phosphorylation in the challenge and is not significantly altered due to BG+MPT; this peptide is involved in the activity of the FAK2 kinase enzyme involving metabolic pathway activation (Kuwabara et al., 2004). In summary, the effect of these phosphorylation changes is to increase cell survival and growth in the treatment group and to inhibit growth and induce cell death in the NE challenge group.

Table 9 shows the peptides that are uniquely significant or are phosphorylated in the opposite direction (i.e., increased in one group, down in the other group) between challenge and BG+MPT treated groups and

Table 9. Peptides in "regulation of apoptotic processes" showing opposite differential phosphorylation relative to control in challenge and BG+MPT.

UniProt ID	ProteinName	Human site	Chicken site	Challenge FC	Challenge *P* value	BG FC	BG *P* value	MPT FC	MPT *P* value	YCW FC	YCW *P* value	BG+MPT FC	BG+MPT *P* value
O96013	PAK4	S474	S283	−1.071	0.001	−1.051	0.035					1.024	0.041
P12931	SRC	S17	S17	1.032	0.037							−1.030	0.016
P14921	ETS1	T38	T82	−1.031	0.013							1.047	0
P31749	AKT1	T308	T74	−1.045	0.020							1.054	0.008
P37231	PPARG	S112	S82	−1.042	0.032							1.084	0
P49840	GSK3A	S278	S185	−1.080	0.004							1.074	0.028
P49841	GSK3B	Y216	Y186	1.075	0.008	1.077	0.001			−1.091	0	−1.056	0.010
P51692	STA5B	Y699	Y700	−1.036	0.003			1.041	0			1.054	0.003
Q13131	AAPK1	S172	S174	−1.052	0.001					−1.022	0.0178	1.032	0.018
Q16654	PDK4	S369	S363	−1.153	0	−1.095	0.001	−1.130	0	−1.105	0	1.029	0.037

A *P*-value of 0.05 was used to determine significance. Non-significant values have been omitted.
Abbreviations: BG, β-glucan; FC, fold change; MPT, mannoproteins; YCW, yeast cells wall.

are members of the "regulation of apoptotic processes" biological process. The complete list of significantly differentially phosphorylated peptides implicated in regulation of apoptotic processes can be found in Supplementary Table 2. We observe that most of the differences between the 2 groups is due to the peptides displaying less phosphorylation relative to control in the challenge group. The changes in phosphorylation of these sites due to challenge affect cellular function in the following ways: Serine/threonine-protein kinase PAK 4 (PAK4) S283 (Human S474) is deactivated on this progrowth site (Callow et al., 2002, p. 4), protein C-ets-1 (ETS1) T82 (Human T38) is deactivated on this progrowth site (Rabault et al., 1996, p. 1), glycogen synthase kinase-3 beta (GSK3B) Y186 (Human Y216) is deactivated on this apoptosis inducer site (Bhat et al., 2000), AKT1 T74 (Human T308) is deactivated on this apoptosis inhibitor site (Koh et al., 2000, p. 2), and transcription factor STAT5B Y700 (Human Y699) is deactivated on its transcription related site (Fox et al., 2008). Taken together, these results show that in the NE challenged jejunum, there is a repression of cell growth and transcription and a mixed apoptotic signaling response. Treatment with BG+MPT reverses these responses.

Table 10 shows the peptides that are uniquely significant or phosphorylated in the opposite direction (i.e., increased in one group, down in the other group) between challenge and BG+MPT treated groups that are members of the "innate immune response-activating signal transduction" biological process. The complete list of significantly differentially phosphorylated peptides implicated in "innate immune response-activating signal transduction" can be found in Supplementary Table 3. In this table, we observe a mixture of increased and reduced phosphorylation in the 2 groups. Looking at the functions of these phosphorylation sites, we see that sites related to cell growth are altered in both challenge and treatment groups, including proto-oncogene c-Src (SRC) (Schmitt and Stork, 2002), ribosomal protein S6 kinase alpha-5 (KS6A5) (Li et al., 2015), and mitogen-activated protein kinase 1 (MK01) (Lawn et al., 2015). Caspase 8 (CASP8) S350 phosphorylation inhibits apoptosis (Alvarado-Kristensson et al., 2004) and is phosphorylated in the treatment group. Again, we see the impact of challenge on cell growth was reversed by the BG+MPT treatment and that apoptosis signaling was inhibited.

Of note is that most of the peptides listed in Tables 8–10 (which are opposite between challenge and BG+MPT) are predominantly related to cell growth and survival. In the challenge group, most peptide phosphorylation function affects are directed at decreasing or shutting down cell growth and inducing cell death, perhaps through apoptotic signals. The BG+MPT treatment reversed many of these phosphorylation changes due to challenge. An

Table 10. Peptides in "innate immune response-activating signal transduction" showing opposite differential phosphorylation relative to control in Challenge and BG+MPT.

UniProt ID	Protien name	Human site	Chicken site	Challenge FC	Challenge *P* value	BG FC	BG *P* value	MPT FC	MPT *P* value	YCW FC	YCW *P* value	BG+MPT FC	BG+MPT *P* value
O75582	KS6A5	T581	T571	−1.036	0.012							1.086	0.001
P12931	SRC	S17	S17	1.032	0.037							−1.030	0.016
P17252	KPCA	T497	T499	−1.032	0.029					−1.055	0	1.025	0.023
P17612	KAPCA	S140	S187	1.034	0.013							−1.070	0
P28482	MK01	T185	T146	1.072	0.007			−1.084	0.005			−1.066	0.017
P36507	MP2K2	S306	S304	1.034	0.006	1.023	0.045	1.042	0.043	1.036	0.001		
Q14790	CASP8	S347	S350	−1.084	0					−1.032	0.020	1.052	0.017

A *P* value of 0.05 was used to determine significance. Nonsignificant values have been omitted.
Abbreviations: BG, β-glucan; FC, fold change; MPT, mannoproteins; YCW, yeast cells wall.

intriguing possibility is that the necrosis of cells observed in NE pathology of the gut may be strongly influenced by the inhibition of cell growth, division, and differentiation rather than the direct killing of the cells by the infection. As necrosis is also an inflammatory process, this may drive the inflammation and further pathology within gut tissue.

While we observed clear differences in the phosphorylation status of key peptides between challenge and BG+MPT treated, often these peptides phosphorylation was not significantly altered in the BG alone, MPT alone, and YCW treatment groups (Tables 8–10). It is possible that the differences in these peptides phosphorylation state are a key aspect of the difference in growth response we observed here, either allowing the disease to take hold and negatively affect growth in the case of the challenge group or reducing disease severity and limiting growth effects in the case of the BG+MPT group. Thus, the lack of significant change in phosphorylation of these specific peptides may be the reason we do not see a significant improvement in growth due to treatment with YWC, BG alone, or MPT alone. In other words, these peptides described previously may be critical determinants of disease severity and the growth effects due to this NE challenge model.

qRT-PCR Cytokine mRNA Transcription

Changes in mRNA expression of both proinflammatory and anti-inflammatory cytokines were also measured between the experimental groups. qRT-PCR was conducted using flash frozen jejunal tissue from birds in the various treatment and control groups. Fold change was then determined using the ΔΔCt method, using the 28S gene as the housekeeping gene and the control uninfected jejunal tissue as a control. Table 11 summarizes the results of this analysis. Many of the genes studied do not show large fold change differences compared to control housekeeping genes and non-challenged birds. However, we can see that several of the genes show large differences in expression magnitude or direction of change (− vs. +) between the challenge group (NE) and the BG+MPT group, including interleukin (IL)-6, IL-10, IL-12β, and interferon (IFN)-α. These changes suggest effects on gene expression in response to the NE challenge and further changes in response to the various treatment groups, rather than a return to control levels of expression. This is consistent with the kinome data (Figure 1) that showed that the various YCW compound treatments did not return the tissue to a control-like kinotype but instead further separated the treated groups from the control and challenge groups.

The interpretation of immune responses in the gut is difficult, especially with gene expression data. This is because there is an active, homeostatic balance between proinflammatory and anti-inflammatory responses continuously occurring in the gut. Often one will see seemingly opposite proinflammatory and anti-inflammatory genes being expressed at the same time, which can confuse interpretation, but one must look at the overall balance to see if it is tipped one way or the other. The changes in proinflammatory and anti-inflammatory cytokines between groups suggest that inflammation is a complex physiological process, not easily characterized by measuring mRNA expression, which by its nature is often a lagging indicator. As the majority of our kinome data interpretation focused on the differences between challenge and BG+MPT treated, we can consider the gene expression data similarly. In doing so, we see that IL-6, IL-10, IL-12β, and IFN-α all show differences in expression between these 2 groups (Table 11). IL-6 is an inflammatory cytokine, and its expression is not changed in the challenge group, while in the BG+MPT group, its expression is decreased −6.7621-fold. This indicates that the treatment has an anti-inflammatory effect in this NE challenge model. IL-10 is often considered anti-inflammatory, it can also be considered immune modulatory as it returns the system to homeostasis after an inflammatory response, and here there is a slight increase in expression in the challenge group and a slight decrease in the BG+MPT group. This may indicate a physiological response attempting to control inflammation in the challenge birds while that would not be required in the treatment group. IL-12β is an immune-activating cytokine that often targets T-cells and natural killer cells, resulting in a cell-mediated immune response. Here we see a slight decrease in expression in the challenge group and a slight increase in the BG+MPT group. This may indicate a predominantly innate inflammatory response in the challenge, while there may be a more cell-based response in the treatment group. Finally, both the challenge

Table 11. mRNA expression fold change (2ˆ-ΔΔCt) of proinflammatory and anti-inflammatory cytokines from jejunal tissue.

Group	IL-1β	IL-6	MIP-1β	IL-10	IL-12α	IL-12β	IL-15	IL-21	IFN-α	IFN-γ	IL-8
NE	1.035	−1.006	−1.315	1.548	−1.627	−1.563	−1.356	2.114	−2.581	−1.394	−1.133
YCW	−2.126	−2.882	−1.312	−6.084	−3.608	1.068	−2.005	1.343	−3.978	−1.391	−2.441
BG	1.097	−2.509	−1.184	−1.188	−2.045	1.070	−2.810	4.263	−1.352	1.051	−1.116
MPT	−2.344	−4.027	−1.290	−7.502	−5.723	1.019	−2.724	1.329	−10.678	−1.873	−2.948
BG+MPT	−1.884	−6.762	−1.554	−2.291	−3.117	1.676	−3.710	2.552	−9.625	−1.360	−2.499

Fold change was calculated using 2ˆ-ΔΔCt method with housekeeping gene being 28S and control RNA from jejunal tissue from uninfected control birds. Fold changes where treatment expression is less than control expression and is thus has been <1-fold change corrected to a negative value.

Abbreviations: BG, β-glucan; IFN, interferon; IL, interleukin; MPT, mannoproteins; NE, necrotic enteritis; YCW, yeast cells wall.

group and the treatment group show a decrease in IFN-α expression, with a larger decrease (−9.62521-fold) in the treatment group. IFN-α is an antiproliferative and immunomodulatory cytokine (Gibbert et al., 2013), and these responses are likely not required in a controlled response situation observed in the treatment group. It is of note that most of the differential phosphorylation-based signaling described previously showed that the BG+MPT treated tissue had more of a cell growth and antiapoptotic response, indicative of low levels of IFN-α.

CONCLUSION

NE is a complex disease that is not fully understood, and further complicating our understanding of NE is that there are multiple methods of experimentally inducing disease pathogenesis. It is entirely possible that NE is a spectrum of symptoms that can be elicited in a variety of ways, a syndrome, rather than a cause-effect linear infectious disease. Here we used a combination of IBDV and *C. perfringens*. We have shown that a combination compound used as a feed additive consisting of purified YCW components, BG+MPT, is able to recover weight gain in NE-challenged birds as well as confer unique cellular signal transduction in the guts of challenged broilers. The responses appear centered on inducing cell growth responses and reducing cell death or apoptosis and innate inflammatory responses, but rather than returning the tissue to a non–challenged-like state, the treatment appears to generate compensatory signaling to reduce disease severity.

ACKNOWLEDGEMENTS

This project was partially funded by Phileo-Lesaffre Animal Care.

The authors report no conflict of interest.

SUPPLEMENTARY DATA

Supplementary data associated with this article can be found in the online version at http://doi.org/10.1016/j.psj.2020.03.012.

REFERENCES

Alvarado-Kristensson, M., F. Melander, K. Leandersson, L. Rönnstrand, C. Wernstedt, and T. Andersson. 2004. p38-MAPK signals survival by phosphorylation of Caspase-8 and Caspase-3 in human neutrophils. J. Exp. Med. 199:449–458.

Annett, C. B., J. R. Viste, M. Chirino-Trejo, H. L. Classen, D. M. Middleton, and E. Simko. 2002. Necrotic enteritis: effect of barley, wheat and corn diets on proliferation of Clostridium perfringens type A. Avian Pathol. 31:598–601.

Arsenault, R., and M. H. Kogut. 2012. Chicken-specific peptide arrays for kinome analysis: Flight for the Flightless. Curr. Top. Biotechnol. 7:79–89.

Arsenault, R. J., J. T. Lee, R. Latham, B. Carter, and M. H. Kogut. 2017. Changes in immune and metabolic gut response in broilers fed β-mannanase in β-mannan-containing diets. Poult. Sci. 96:4307–4316.

Bhat, R. V., J. Shanley, M. P. Correll, W. E. Fieles, R. A. Keith, C. W. Scott, and C.-M. Lee. 2000. Regulation and localization of tyrosine 216 phosphorylation of glycogen synthase kinase-3β in cellular and animal models of neuronal degeneration. Proc. Natl. Acad. Sci. U. S. A. 97:11074–11079.

Callow, M. G., F. Clairvoyant, S. Zhu, B. Schryver, D. B. Whyte, J. R. Bischoff, B. Jallal, and T. Smeal. 2002. Requirement for PAK4 in the Anchorage-independent growth of human cancer cell lines. J. Biol. Chem. 277:550–558.

Choct, M., and G. Annison. 1992. The inhibition of nutrient digestion by wheat pentosans. Br. J. Nutr. 67:123–132.

Cohen, R. E., and C. E. Ballou. 1981. Mannoproteins: structure. Pages 441–458 in Plant Carbohydrates II: Extracellular Carbohydrates. W. Tanner and F. A. Loewus eds, Encyclopedia of Plant Physiology. Springer Berlin Heidelberg, Berlin, Heidelberg.

Cooper, K. K., and J. G. Songer. 2009. Necrotic enteritis in chickens: a paradigm of enteric infection by Clostridium perfringens type A. Anaerobe 15:55–60.

Cox, C. M., L. H. Stuard, S. Kim, A. P. McElroy, M. R. Bedford, and R. A. Dalloul. 2010. Performance and immune responses to dietary β-glucan in broiler chicks. Poult. Sci. 89:1924–1933.

Fox, E. M., T. M. Bernaciak, J. Wen, A. M. Weaver, M. A. Shupnik, and C. M. Silva. 2008. Signal transducer and activator of transcription 5b, c-Src, and epidermal growth factor receptor signaling play integral roles in estrogen-stimulated proliferation of estrogen receptor-positive breast cancer cells. Mol. Endocrinol. Baltim. Md. 22:1781–1796.

Gibbert, K., J. F. Schlaak, D. Yang, and U. Dittmer. 2013. IFN-α subtypes: distinct biological activities in anti-viral therapy. Br. J. Pharmacol. 168:1048–1058.

Ha, C. H., C.-W. Yun, H. D. Paik, S. W. Kim, C. W. Kang, H. J. Hwang, and H.-I. Chang. 2006. Preparation and analysis of yeast cell wall mannoproteins, immune enchancing materials, from cell wall mutant Saccharomyces cerevisiae. J. Microbiol. Biotechnol. 16:247–255.

Hashim, M. M., R. J. Arsenault, J. A. Byrd, M. H. Kogut, M. Al-Ajeeli, and C. A. Bailey. 2018. Influence of different yeast cell wall preparations and their components on performance and immune and metabolic pathways in Clostridium perfringens-challenged broiler chicks. Poult. Sci. 97:203–210.

Hunter, T. 1995. Protein kinases and phosphatases: the Yin and Yang of protein phosphorylation and signaling. Cell 80:225–236.

Iji, P. A., A. A. Saki, and D. R. Tivey. 2001. Intestinal structure and function of broiler chickens on diets supplemented with a mannan oligosaccharide. J. Sci. Food Agric. 81:1186–1192.

Immerseel, F. V., J. D. Buck, F. Pasmans, G. Huyghebaert, F. Haesebrouck, and R. Ducatelle. 2004. Clostridium perfringens in poultry: an emerging threat for animal and public health. Avian Pathol. 33:537–549.

Jalal, S., R. Arsenault, A. A. Potter, L. A. Babiuk, P. J. Griebel, and S. Napper. 2009. Genome to kinome: species-specific peptide arrays for kinome analysis. Sci. Signal. 2:pl1.

Jalal, S., J. Kindrachuk, and S. Napper. 2007. Phosphoproteome and kinome analysis: unique perspectives on the same problem. Curr. Anal. Chem. 3:1–15.

Kaiser, P., L. Rothwell, E. E. Galyov, P. A. Barrow, J. Burnside, and P. Wigley. 2000. Differential cytokine expression in avian cells in response to invasion by Salmonella typhimurium, Salmonella enteritidis and Salmonella gallinarum. Microbiology 146:3217–3226.

Kaldhusdal, M., M. Hofshagen, A. Løvland, H. Langstrand, and K. Redhead. 1999. Necrotic enteritis challenge models with broiler chickens raised on litter: evaluation of preconditions, Clostridium perfringens strains and outcome variables. FEMS Immunol. Med. Microbiol. 24:337–343.

Kanehisa, M., M. Furumichi, M. Tanabe, Y. Sato, and K. Morishima. 2017. KEGG: new perspectives on genomes, pathways, diseases and drugs. Nucleic Acids Res. 45:D353–D361.

Kebache, S., E. Cardin, D. T. Nguyên, E. Chevet, and L. Larose. 2004. Nck-1 Antagonizes the Endoplasmic Reticulum stress-induced inhibition of translation. J. Biol. Chem. 279:9662–9671.

Kogut, M. H., L. Rothwell, and P. Kaiser. 2003. Differential regulation of cytokine gene expression by avian Heterophils during receptor-mediated Phagocytosis of Opsonized and Nonopsonized Salmonella enteritidis. J. Interferon Cytokine Res. 23:319–327.

Koh, H., K. H. Lee, D. Kim, S. Kim, J. W. Kim, and J. Chung. 2000. Inhibition of akt and its anti-apoptotic activities by Tumor necrosis factor-induced protein kinase C-related kinase 2 (PRK2) Cleavage. J. Biol. Chem. 275:34451–34458.

Kuwabara, K., T. Nakaoka, K. Sato, T. Nishishita, T. Sasaki, and N. Yamashita. 2004. Differential regulation of cell Migration and proliferation through Proline-Rich tyrosine kinase 2 in Endothelial cells. Endocrinology 145:3324–3330.

Lawn, S., N. Krishna, A. Pisklakova, X. Qu, D. A. Fenstermacher, M. Fournier, F. D. Vrionis, N. Tran, J. A. Chan, R. S. Kenchappa, and P. A. Forsyth. 2015. Neurotrophin signaling via TrkB and TrkC receptors Promotes the growth of Brain Tumor-initiating cells. J. Biol. Chem. 290:3814–3824.

Lee, K. W., H. S. Lillehoj, W. Jeong, H. Y. Jeoung, and D. J. An. 2011. Avian necrotic enteritis: experimental models, host immunity, pathogenesis, risk factors, and vaccine development. Poult. Sci. 90:1381–1390.

Li, B., Z. Wan, G. Huang, Z. Huang, X. Zhang, D. Liao, S. Luo, and Z. He. 2015. Mitogen- and stress-activated Kinase 1 mediates Epstein-Barr virus latent membrane protein 1-promoted cell transformation in nasopharyngeal carcinoma through its induction of Fra-1 and c-Jun genes. BMC Cancer 15:390.

Lipke, P. N., and R. Ovalle. 1998. Cell wall Architecture in yeast: new structure and new challenges. J. Bacteriol. 180:3735–3740.

Lovland, A., and M. Kaldhusdal. 2001. Severely impaired production performance in broiler flocks with high incidence of Clostridium perfringens-associated hepatitis. Avian Pathol. J. WVPA 30:73–81.

Ma, K., S. M. Cheung, A. J. Marshall, and V. Duronio. 2008. PI(3,4,5) P3 and PI(3,4)P2 levels correlate with PKB/akt phosphorylation at Thr308 and Ser473, respectively; PI(3,4)P2 levels determine PKB activity. Cell. Signal. 20:684–694.

McReynolds, J. L., J. A. Byrd, R. C. Anderson, R. W. Moore, T. S. Edrington, K. J. Genovese, T. L. Poole, L. F. Kubena, and D. J. Nisbet. 2004. Evaluation of immunosuppressants and dietary mechanisms in an experimental disease model for necrotic enteritis. Poult. Sci. 83:1948–1952.

M'Sadeq, S. A., S.-B. Wu, M. Choct, R. Forder, and R. A. Swick. 2015. Use of yeast cell wall extract as a tool to reduce the impact of necrotic enteritis in broilers. Poult. Sci. 94:898–905.

National Research Council (US) Committee for the Update of the Guide for the Care and Use of Laboratory Animals 2011. Guide for the Care and Use of Laboratory Animals, 8th ed. National Academies Press (US), Washington (DC).

Novak, M., and V. Vetvicka. 2008. β-Glucans, history, and the present: immunomodulatory aspects and mechanisms of action. J. Immunotoxicol. 5:47–57.

Pietrella, D., G. Bistoni, C. Corbucci, S. Perito, and A. Vecchiarelli. 2006. Candida albicans mannoprotein influences the biological function of dendritic cells. Cell. Microbiol. 8:602–612.

Postigo, A., A. M. Calella, B. Fritzsch, M. Knipper, D. Katz, A. Eilers, T. Schimmang, G. R. Lewin, R. Klein, and L. Minichiello. 2002. Distinct requirements for TrkB and TrkC signaling in target innervation by sensory neurons. Genes Dev. 16:633–645.

Rabault, B., M. F. Roussel, C. T. Quang, and J. Ghysdael. 1996. Phosphorylation of Ets1 regulates the complementation of a CSF-1 receptor impaired in mitogenesis. Oncogene 13:877–881.

Sarson, A. J., Y. Wang, Z. Kang, S. E. Dowd, Y. Lu, H. Yu, Y. Han, H. Zhou, and J. Gong. 2009. Gene expression profiling within the spleen of Clostridium perfringens- challenged Broilers fed antibiotic-medicated and non-medicated diets. BMC Genomics 10:260.

Schmitt, J. M., and P. J. S. Stork. 2002. Gα and Gβγ Require distinct Src-dependent pathways to activate Rap1 and Ras. J. Biol. Chem. 277:43024–43032.

Shimizu, T., K. Ohtani, H. Hirakawa, K. Ohshima, A. Yamashita, T. Shiba, N. Ogasawara, M. Hattori, S. Kuhara, and H. Hayashi. 2002. Complete genome sequence of Clostridium perfringens, an anaerobic flesh-eater. Proc. Natl. Acad. Sci. 99:996–1001.

Soltanian, S., E. Stuyven, E. Cox, P. Sorgeloos, and P. Bossier. 2009. Beta-glucans as immunostimulant in vertebrates and invertebrates. Crit. Rev. Microbiol. 35:109–138.

Songer, J. G. 1996. Clostridial enteric diseases of domestic animals. Clin. Microbiol. Rev. 9:216–234.

Swaggerty, C. L., I. Y. Pevzner, P. Kaiser, and M. H. Kogut. 2008. Profiling pro-inflammatory cytokine and chemokine mRNA expression levels as a novel method for selection of increased innate immune responsiveness. Vet. Immunol. Immunopathol. 126:35–42.

Szklarczyk, D., A. Franceschini, S. Wyder, K. Forslund, D. Heller, J. Huerta-Cepas, M. Simonovic, A. Roth, A. Santos, K. P. Tsafou, M. Kuhn, P. Bork, L. J. Jensen, and C. von Mering. 2015. STRING v10: protein-protein interaction networks, integrated over the tree of life. Nucleic Acids Res. 43:D447–D452.

Teirlynck, E., L. Bjerrum, V. Eeckhaut, G. Huygebaert, F. Pasmans, F. Haesebrouck, J. Dewulf, R. Ducatelle, and F. Van Immerseel. 2009. The cereal type in feed influences gut wall morphology and intestinal immune cell infiltration in broiler chickens. Br. J. Nutr. 102:1453–1461.

Trost, B., J. Kindrachuk, P. Määttänen, S. Napper, and A. Kusalik. 2013. Piika 2: an Expanded, Web-based platform for analysis of kinome microarray data. PLoS ONE 8:e80837.

Wade, B., and A. Keyburn. 2015. The True Cost of Necrotic Enteritis. PoultryWorld. Accessed Oct. 2019. https://www.poultryworld.net/Meat/Articles/2015/10/The-true-cost-of-necrotic-enteritis-2699819W/.

Yuan, J. S., A. Reed, F. Chen, and C. N. Stewart. 2006. Statistical analysis of real-time PCR data. BMC Bioinformatics 7:85.